Al-Farouk journal of sciences
Volume (2), Issue (3) (JUNE, 2026)
ISSN: 3135-2359

مجلة الفاروق للعلوم
المجلد (2) العدد 3 يونيو 2026
ردمد: 3135-2359

Finite-Control-Set Model Predictive Direct Power Control of Grid-Connected Photovoltaic Inverters

Fouad Mohamed Eltoumi[1*], Said Ahmed[2], Tawfiq Alhamisi[3]
[1*,2] The Higher Institute of Science and Technology, Riqdalin, Libya.
Corresponding author: eltoumifouad@gmail.com

تاريخ الاستلام: 2026/04/21 تاريخ المراجعة 23/05/ 2026 تاريخ القبول:2026/06/07- تاريخ النشر: 30/06/ 2026

Abstract: This paper proposes a model predictive direct power control strategy for photovoltaic grid-connected inverters based on instantaneous power theory in a rotating d-q reference frame. This method shows a discrete power prediction model using sampled grid voltage and current, directly predicting the inverter's future active and reactive power without requiring an internal current control loop or a pulse width modulation stage. A finite control set model predictive control algorithm is used to evaluate the available inverter voltage vector. The optimal switching vector is selected by minimizing a cost function that defined as the sum of the absolute tracking errors between the predicted and reference active power and the reference active and reactive power. To verify the effectiveness of the proposed control method, simulation studies were conducted under different operating conditions, including step changes in active and reactive power and fluctuations in solar irradiance. The results show that the photovoltaic grid-connected inverter attains fast power point tracking with reduction in control complexity, and adequate steady-state and dynamic performance. These results verify that the proposed model predictive direct power control strategy is a feasible and effective solution for improving the dynamic response and control performance of photovoltaic grid-connected inverter systems.

Keywords: Photovoltaic system; Grid-connected inverter; Model predictive control; d-q reference frame.

1. Introduction

The growing demand for clean and sustainable electric energy has accelerated the utilization of renewable energy generation systems, especially photovoltaic (PV) power generation. PV systems are widely used due to their modular structure, environmental benefits, low maintenance requirements, and suitability for distributed generation. However, large-scale PV power generation integrated into the grid presents many technical challenges, including power quality, dynamic response, grid synchronization, and active/reactive power regulation. Therefore, the grid-connected inverter plays a key role as the interface between the PV array and the AC grid, and its control performance directly affects the stability and quality of the injected power [1][2].

In a grid-connected PV system, the inverter is responsible for converting the DC power generated by the PV array into AC power that meets the grid requirements. To achieve this purpose, the controller must make certain fast active power (P) tracking, accurate reactive power (Q) control, low current distortion, and stable operation under different solar irradiance conditions. Due to the rapid changes in solar irradiance and temperature, the inverter control system should provide dynamic performance while maintaining satisfactory steady-state accuracy [3]. Conventional grid-connected inverter control methods include voltage-oriented control, dual-loop PI control, hysteresis current control, and deadbeat control [4]–[6]. Although these methods have been widely used, each method has certain limitations. For example, PI-based dual-loop control requires fine parameter tuning and usually relies on internal current loops and pulse width modulation (PWM). Hysteresis control has a fast response speed. However, this control suffers from unstable switching frequency. Deadbeat control has a simple structure and fast transient response. However, its performance is sensitive to changes in system parameters [6],[7]. In recent years, model predictive control (MPC) has concerned widespread attention in power electronics and renewable energy systems. MPC uses a mathematical model of the system to predict its future behavior and then selects the optimal control action by minimizing a predefined cost function. Compared with conventional linear controllers, MPC has many advantages, including fast dynamic response, simple digital implementation, direct consideration of system constraints, and the ability to handle multivariable control problems [8],[9]. In particular, finite set MPC (FCS-MPC) is well-compatible for voltage source inverters due to the ability to directly assess the switching state of the converter without requiring a separate PWM stage [10]. This characteristic makes FCS-MPC highly attractive in grid-connected inverter applications that require fast response and simplified control structures.

MPC has been applied to various inverter control strategies, such as model predictive current control and model predictive direct power control (MPDPC). In model predictive current control, the grid current component is predicted and directly controlled in a stationary αβ coordinate system or a rotating d-q coordinate system. However, in grid-connected photovoltaic applications, the primary control aims are usually active power injection and reactive power regulation. Therefore, MPDPC is more suitable because it directly regulates active and reactive power, rather than controlling the current as an intermediate variable as in traditional methods [11][12]. Traditional direct power control methods are typically employed in a stationary αβ reference system. While this approach reduces computational complexity, it may not achieve ideal decoupling between active and reactive power, especially under transient conditions [13].

To overcome these limitations, this paper proposes a MPDPC strategy for grid-connected PV inverters based on a rotating d-q coordinate system. Utilizing instantaneous power theory, a power prediction model is established to directly estimate future active and reactive power based on sampled grid voltage and current. At each sampling time, all voltage vectors of the inverter are evaluated, and the optimal vector is selected by minimizing a cost function. This cost function is defined as the sum of the absolute errors between the predicted and reference active and reactive power. Unlike traditional control methods, the proposed method does not require an internal current control loop or PWM, thus simplifying the control structure and reducing implementation complexity.

The main contribution of this paper is the proposal of a simple and effective MPDPC strategy for PV grid-connected inverters in a rotating d-q reference system. This method improves the decoupling capability between active and reactive power while maintaining fast response.

2. Mathematical Model for Power Prediction of Grid-Connected Photovoltaic Inverter

Figure 1 shows a single-stage three-phase grid-connected photovoltaic inverter [14]. The inverter is connected to the grid through a filter inductor L and a line resistance R. According to Kirchhoff's laws, the state equation of the system in the three-phase stationary coordinate system is shown in equation (1) [14].

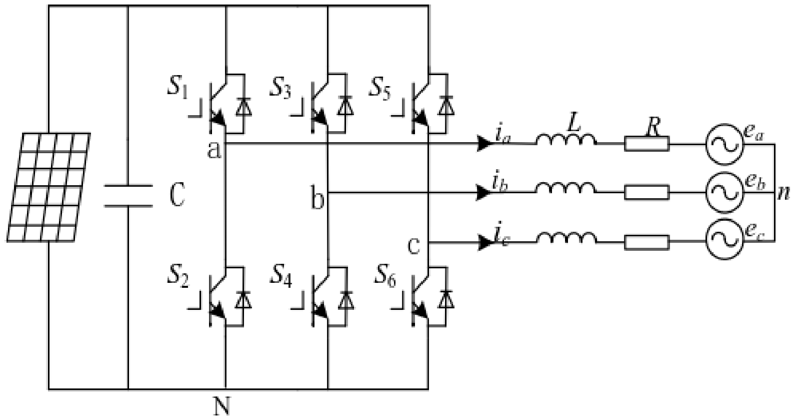

Fig.1: Three phase Grid-connected Photovoltaic inverter.

$$L\frac{d}{dt}\begin{bmatrix} i_a \\ i_b \\ i_c \end{bmatrix} + R\begin{bmatrix} i_a \\ i_b \\ i_c \end{bmatrix} + \begin{bmatrix} e_a \\ e_b \\ e_c \end{bmatrix} = \begin{bmatrix} u_{aN} \\ u_{bN} \\ u_{cN} \end{bmatrix} \quad (1)$$

where L is the filter inductance, R is the filter resistance, i_a, i_b, and $i_c$are the three-phase grid currents, e_a, e_b, and $e_c$are the three-phase grid voltages, and u_{aN}, u_{bN}, and $u_{cN}$are the inverter output phase voltages with respect to the neutral point N.

The relationship between the inverter bridge-arm voltages and the phase voltages can be written as:

$$\begin{bmatrix} u_{aN} \\ u_{bN} \\ u_{cN} \end{bmatrix} = \begin{bmatrix} u_{an} \\ u_{bn} \\ u_{cn} \end{bmatrix} - \begin{bmatrix} u_{Nn} \\ u_{Nn} \\ u_{Nn} \end{bmatrix} \quad (2)$$

where u_{an}, u_{bn}, and $u_{cn}$are the inverter bridge voltages with respect to the DC-bus midpoint n, and $u_{Nn}$is the voltage difference between the grid neutral point $N$and the DC-bus midpoint n.

By applying the Park transformation to equation (1), the state equation under the dd-qq rotating coordinates is shown in equation (3) [14], [15].

$$L\frac{d}{dt}\begin{bmatrix} i_d \\ i_q \end{bmatrix} + \begin{bmatrix} R & -\omega L \\ \omega L & R \end{bmatrix}\begin{bmatrix} i_d \\ i_q \end{bmatrix} + \begin{bmatrix} e_d \\ e_q \end{bmatrix} = \begin{bmatrix} u_d \\ u_q \end{bmatrix} \quad (3)$$

where $i_d$and $i_q$are the grid-current components in the rotating dq coordinate system, $e_d$and $e_q$are the grid-voltage components, and u_d and u_q are the inverter output-voltage components in the same reference frame. The parameter ω represents the grid angular frequency. This equation describes the dynamic model of the grid-connected inverter after transforming the three-phase abc model into the synchronous rotating dq frame.

The three-phase photovoltaic grid-connected inverter shown in Figure 1, has 7 different voltage vectors, and the resulting voltage space vector [14], [16] as shown in Figure 2.

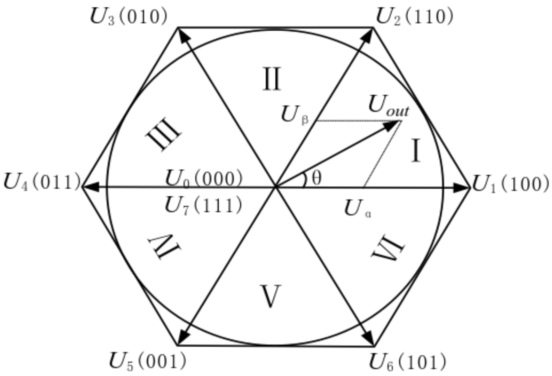

Fig 2: Inverter voltage space vector.

Define the switching states Si (i=a,b,c) of a three-phase photovoltaic grid-connected inverter as follows:

$$S_i = \begin{cases} 1, & \text{upper switch of phase } i \text{ is ON and lower switch is OFF} \\ 0, & \text{upper switch of phase } i \text{ is OFF and lower switch is ON} \end{cases} \qquad (4)$$

where S_{ib} represents the switching state of phase i, and $i$can be phase a, b, or c. When $S_i = 1$, the upper switch of the corresponding inverter leg is conducting, while the lower switch is turned off. When $S_i = 0$, the upper switch is turned off, while the lower switch is conducting.

The output voltage Ui (i=d,q) of the grid-connected inverter is:

$$\begin{bmatrix} u_d \\ u_q \end{bmatrix} = \frac{2}{3}\begin{bmatrix} \cos\theta & \sin\theta \\ -\sin\theta & \cos\theta \end{bmatrix}\begin{bmatrix} 1 & -\frac{1}{2} & -\frac{1}{2} \\ 0 & \frac{\sqrt{3}}{2} & -\frac{\sqrt{3}}{2} \end{bmatrix}\begin{bmatrix} S_a U_{dc} \\ S_b U_{dc} \\ S_c U_{dc} \end{bmatrix}$$

where u_d and u_q are the inverter output-voltage components in the rotating dqreference frame, θ is the grid voltage phase angle obtained from the phase-locked loop, and S_a, S_b, and S_c are the switching states of the inverter. The term U_{dc} is the DC-bus voltage. This equation combines the Clarke transformation and Park transformation to convert the inverter switching states into the corresponding voltage vector in the synchronous rotating dqcoordinate system.

Since the resistance R is small, then the R can be ignored, and Equation (3) can be rewritten to obtain:

$$L\frac{d}{dt}\begin{bmatrix} i_d \\ i_q \end{bmatrix} = \begin{bmatrix} u'_d \\ u'_q \end{bmatrix} - \begin{bmatrix} e_d \\ e_q \end{bmatrix} \qquad (6)$$

where the modified inverter voltage components $u'_d$and u'_q are defined as:

$$\begin{bmatrix} u'_d \\ u'_q \end{bmatrix} = \begin{bmatrix} u_d \\ u_q \end{bmatrix} + \begin{bmatrix} \omega L i_d \\ -\omega L i_q \end{bmatrix} \qquad (7)$$

After transforming the inverter model into the synchronous rotating dqreference frame, coupling terms appear between the d-axis and q-axis current components. To simplify the prediction model, the equivalent voltage variables $u'_d$and u'_q are introduced. By incorporating the coupling terms into the inverter voltage components, the current dynamic equation can be rewritten in a simplified form, as shown in Equations (6) and (7). This formulation provides a convenient basis for deriving the active and reactive power prediction model used in the proposed MPDPC strategy.

According to instantaneous power theory [15], in the synchronous rotating dq reference frame, the instantaneous active power $P$and reactive power $Q$of the three-phase photovoltaic grid-connected inverter can be expressed as:

$$\begin{bmatrix} P \\ Q \end{bmatrix} = \frac{3}{2}\begin{bmatrix} e_d & e_q \\ e_q & -e_d \end{bmatrix}\begin{bmatrix} i_d \\ i_q \end{bmatrix} \qquad (8)$$

where $P$is the instantaneous active power, Q is the instantaneous reactive power, $e_d$and $e_q$are the grid-voltage components in the rotating dqcoordinate system, and $i_d$and $i_q$are the grid-current components in the same coordinate system.

Equivalently, Equation (8) can be expanded as:

$$P = \frac{3}{2}(e_d i_d + e_q i_q)$$
$$Q = \frac{3}{2}(e_q i_d - e_d i_q)$$

This equation relates the grid-current components directly with the active and reactive power outputs, which forms the basis for the proposed MPDPC strategy.

By discretizing Equation (6) using the forward Euler method [14], [16], the following expression is obtained:

$$\frac{L}{T_s}\begin{bmatrix} i_d(k+1) - i_d(k) \\ i_q(k+1) - i_q(k) \end{bmatrix} = \begin{bmatrix} u'_d(k) \\ u'_q(k) \end{bmatrix} - \begin{bmatrix} e_d(k) \\ e_q(k) \end{bmatrix} \qquad (9)$$

where $T_s$is the sampling period, $k$is the present sampling instant, and $k+1$is the next sampling instant.

Combining Equation (9) with the equivalent voltage relationship in Equation (7), the current prediction model in the rotating dqcoordinate system can be written as:

$$\frac{L}{T_s}\begin{bmatrix} i_d(k+1) - i_d(k) \\ i_q(k+1) - i_q(k) \end{bmatrix} = \begin{bmatrix} u_d(k) + \omega L i_q(k) - e_d(k) \\ u_q(k) - \omega L i_d(k) - e_q(k) \end{bmatrix} \qquad (10)$$

Equivalently, Equation (10) can be written in expanded form as:

$$i_d(k+1) = i_d(k) + \frac{T_s}{L}[u_d(k) + \omega L i_q(k) - e_d(k)]$$
$$i_q(k+1) = i_q(k) + \frac{T_s}{L}[u_q(k) - \omega L i_d(k) - e_q(k)]$$

Equation (9) represents the discrete form of the inverter current dynamic model. By applying the forward Euler approximation, the derivative of the current is replaced by the difference between the predicted current at the next sampling instant and the measured current at the present instant. Then, by substituting the equivalent voltage components, the prediction equations of $i_d(k+1)$and $i_q(k+1)$ are obtained, as shown in Equation (10). These predicted current components are later used to calculate the predicted active and reactive powers in the proposed MPDPC algorithm.

By discretizing Equation (8), the variation of active and reactive power between the present sampling instant $k$and the next sampling instant $k+1$ can be expressed as:

$$\begin{bmatrix} P(k+1)-P(k) \\ Q(k+1)-Q(k) \end{bmatrix} = \frac{3}{2}\begin{bmatrix} e_d & e_q \\ e_q & -e_d \end{bmatrix}\begin{bmatrix} i_d(k+1)-i_d(k) \\ i_q(k+1)-i_q(k) \end{bmatrix} \tag{11}$$

where $P(k)$and $Q(k)$are the measured active and reactive power at the present sampling instant, while $P(k+1)$and $Q(k+1)$are the predicted active and reactive power at the next sampling instant.

Substituting the discrete current prediction model of Equation (10) into Equation (11), the following power prediction model is obtained:

$$\begin{bmatrix} P(k+1) \\ Q(k+1) \end{bmatrix} = \begin{bmatrix} P(k) \\ Q(k) \end{bmatrix} + \frac{3T_s}{2L}\begin{bmatrix} e_d & e_q \\ e_q & -e_d \end{bmatrix}\begin{bmatrix} u_d(k)+\omega L i_q(k)-e_d(k) \\ u_q(k)-\omega L i_d(k)-e_q(k) \end{bmatrix} \tag{12}$$

Equivalently, Equation (12) can be expanded as:

$$P(k+1) = P(k) + \frac{3T_s}{2L}[e_d(u_d(k)+\omega L i_q(k)-e_d(k))|e_q(u_q(k)-\omega L i_d(k)-e_q(k))]$$
$$Q(k+1) = Q(k) + \frac{3T_s}{2L}[e_q(u_d(k)+\omega L i_q(k)-e_d(k))|e_d(u_q(k)-\omega L i_d(k)-e_q(k))]$$

Equation (12) is the prediction function of the proposed MPDPC for the photovoltaic grid-connected inverter. It predicts the active and reactive power at the next sampling instant using the measured grid voltage, grid current, present active/reactive power, and the candidate inverter voltage vector [14], [17]. Therefore, by evaluating Equation (12) for each switching state of the inverter, the controller can select the voltage vector that gives the smallest power tracking error.

3. The Principle of the Model Predictive Control

The principle of MPC is shown in figure 3. At the sampling instant t_k, the present value of the controlled variable is measured as $x(k)$. According to the discrete prediction model of the system, different control actions $S_1, S_2, S_3, \ldots, S_n$ are applied in the prediction process [17], [18]. As a result, several possible predicted values of the controlled variable at the next sampling instant can be obtained, namely:

$$x_0(k+1),\ x_1(k+1),\ x_2(k+1),\ \ldots,\ x_n(k+1)$$

These predicted values correspond to the possible future trajectories produced by the different switching states. Then, each predicted value is compared with the reference value x^*. The switching state that makes the predicted value closest to the reference value is selected as the optimal switching state.

As illustrated in Figure 3, at time t_k, the predicted value $x_1(k+1)$is the closest one to the reference value x^*. Therefore, the switching action S_2, which produces this predicted value, is selected and applied to the system during the next sampling period T_s, from $t_k$to t_{k+1}.

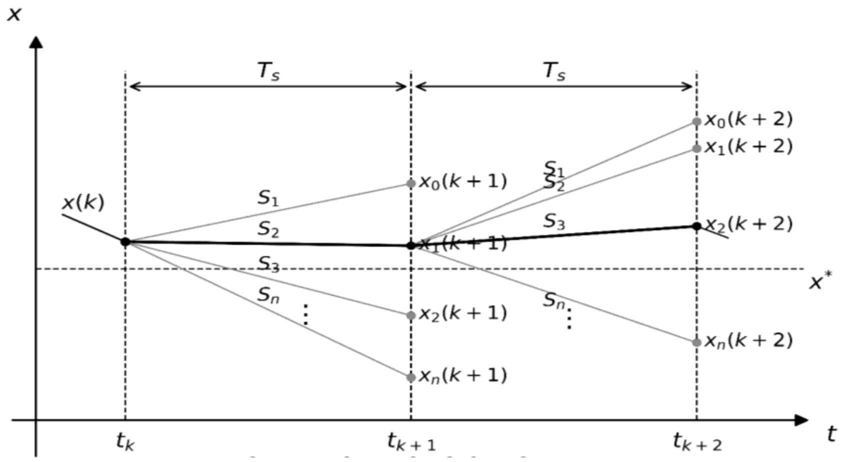

Fig.3 The principle of MPC.

At the next sampling instant t_{k+1}, the controlled variable is measured again. The new measured value becomes the starting point for the next prediction process. Then, the controller again evaluates all switching actions $S_1, S_2, S_3, \ldots, S_n$, and predicts the future values of the controlled variable at t_{k+2}:

$$x_0(k+2),\ x_1(k+2),\ x_2(k+2),\ \ldots,\ x_n(k+2)$$

From the predicted values shown in Fig. 3, $x_2(k+2)$is the closest value to the reference x^*. Therefore, the corresponding switching action $S_3$is selected and applied during the following sampling period. In this way, the controller continuously predicts the future behavior of the system, compares the predicted values with the reference value, and applies only the optimal switching action at each sampling instant.

This repeated prediction and optimization process is defined as the receding-horizon principle. Although several possible future trajectories are predicted, only the first optimal switching action is applied. At the next sampling instant, the prediction is updated using the newly measured system variable [18]. Therefore, MPC can provide fast dynamic response and good tracking performance.

For the photovoltaic grid-connected inverter, the controlled variables are the active power $P$and reactive power Q. The possible control actions are the inverter switching states. At each sampling instant, the controller predicts $P(k+1)$and $Q(k+1)$for all voltage vectors. Then, the predicted powers are compared with the reference values $P^*$and Q^*through the cost function:

$$g = \mid P^* - P(k+1) \mid + \mid Q^* - Q(k+1) \mid \qquad (13)$$

The switching state corresponding to the minimum value of g is selected as the optimal switching state and is directly applied to the inverter [14], [17]. Thus, the proposed MPDPC strategy can directly control the active and reactive powers without using a PWM modulation module or an inner current control loop.

In more detail, the control structure of the proposed model predictive direct power control strategy is shown in Figure 4. The photovoltaic array supplies DC power to the grid-connected inverter through the DC-bus capacitor. The inverter is connected to the three-phase grid through an L-filter with internal resistance R. The three-phase grid voltages e_a, e_b, and e_c, and the grid currents i_a, i_b, and i_c, are sampled and transformed into the synchronous rotating dqreference frame using the transformation. As a result, the voltage components e_d, e_q, and current components i_d, i_q, are obtained.

These dq-axis variables are used as inputs to the power prediction function. The prediction function calculates the predicted active power $P(k+1)$and reactive power $Q(k+1)$for each inverter switching state. Meanwhile, active power reference P^* is generated by the MPPT algorithm according to the available photovoltaic power, while the reactive power reference $Q^*$is set according to the grid operation requirement, usually $Q^* = 0$ for unity power factor operation.

The predicted powers $P(k+1)$ and $Q(k+1)$ are compared with their reference values $P^*$and Q^*in the cost function. The cost function evaluates the tracking error for each candidate voltage vector and selects the switching state that produces the minimum error. The optimal switching signals S_a, S_b, and S_c are then directly applied to the inverter power switches. Therefore, the proposed MPDPC strategy eliminates the need for an inner current control loop and PWM modulation, resulting in a simpler control structure and faster dynamic response.

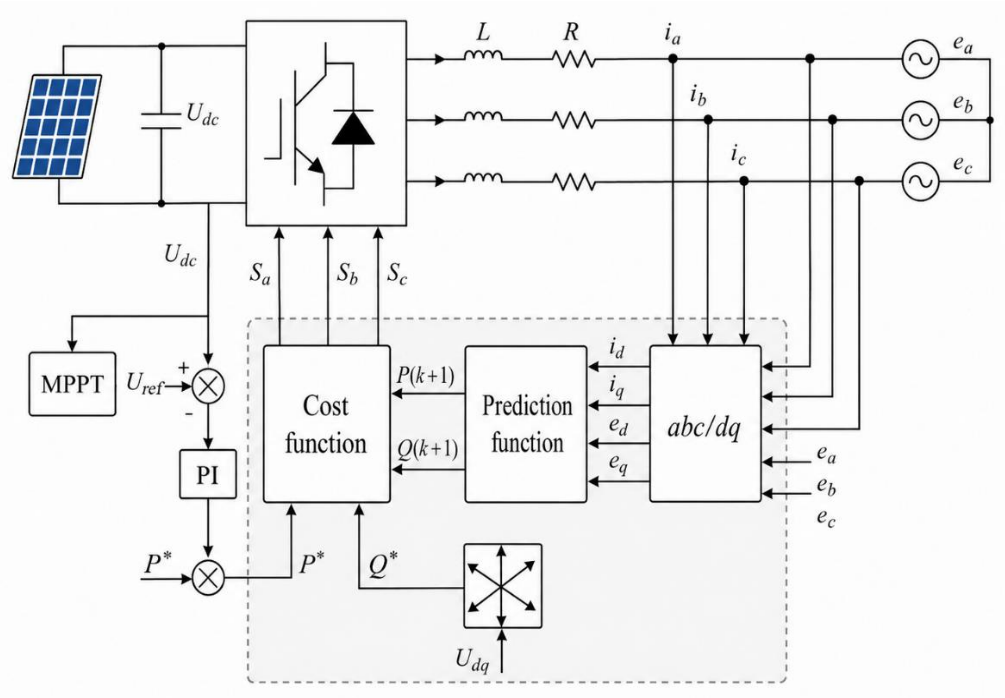

Fig. 4: control structure of the proposed MPDPC strategy.

Generally, the direct power control algorithm is predicted based on the three-phase photovoltaic grid-connected inverter model [14]-[17], and its algorithm flow is shown in Figure 5.

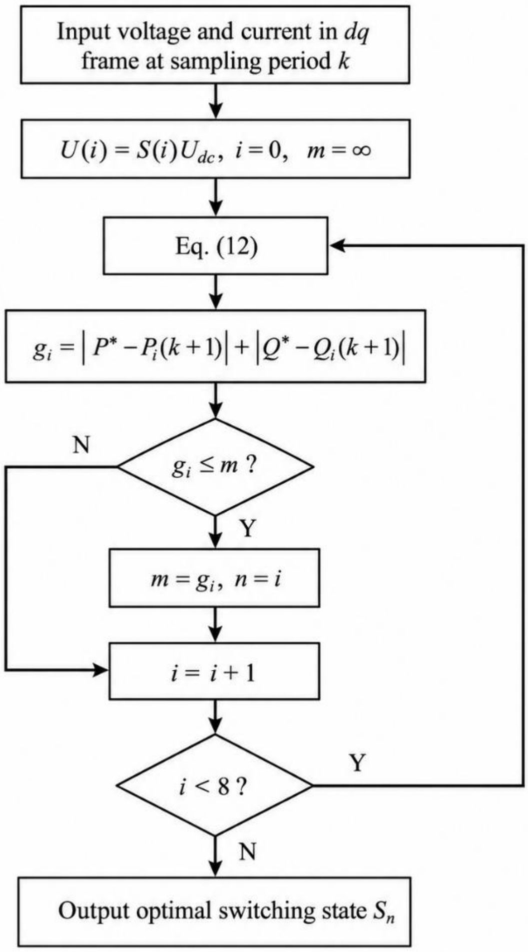

Fig.5 Flow diagram of model MPDPC algorithm.

4. Simulation Results and Discussion

The effectiveness of the MPDPC strategy is evaluated through a series of simulation cases on inverters connected to the photovoltaic grid. These simulations aim to evaluate the dynamic characteristics, steady-state tracking accuracy, active/reactive power decoupling capability, and inverter current characteristics under different operating conditions. The main parameters used in the simulation are DC-bus voltage is $U_{dc} = 380$ V, grid frequency is 50 Hz, grid phase voltage amplitude is 150 V, filter inductance is $L = 15$ mH, and frequency is 20 kHz. The PV array rated power is 5 kW.

Three operating cases were verified in three simulation cases. In Case 1, the active power reference value gradually changed, while the reactive power reference value was set to zero. In Case 2, the reactive power reference value gradually changed, while the active power reference value was set to zero. In Case 3, the irradiance was varied to evaluate the inverter's response under different photovoltaic power generation conditions.

Case 1: Active Power Tracking at $Q^* = 0$

Under the first operating condition, the aim was to evaluate the dynamic tracking capability of the proposed Model Predictive Direct Power Control (MPDPC) strategy for active power.

The DC bus voltage was kept constant at 380V, and the transient response characteristics of the photovoltaic grid-connected inverter were examined by gradually changing the active power reference value. Specifically, within the time period $0 \le t < 0.03$ s, the active power reference value is set to $P^* = 1$ kw; within $0.03 \le t < 0.06$ s, it increases to $P^* = 2$ kw; and within $0.06 \le t \le 0.10$ s, it further increases to $P^* = 3$ kw. To ensure the inverter operates at unity power factor, the reactive power reference value is always set to $Q^* = 0$ throughout the simulation. Other system and controller parameters remain unchanged. The corresponding simulation results are shown in Figures 6(a) and 6(b).

Figure 6(a) shows the dynamic response waveforms of active power P, reactive power Q and their reference values P*, while Figure 6(b) shows the waveforms of the three-phase grid-connected currents ia, ib and ic.

From Figure 6(a), the output active power accurately tracks the reference value command under the three different power levels. When the active power reference value sets from 1 kw to 2 kw at t = 0.03 s, the controller responds quickly and adjusts the actual active power to the new reference value. Similarly, when the active power jumps from 2 kw to 3 kw at t = 0.06 s, the active power also quickly reaches a new steady-state value after a brief transient process.

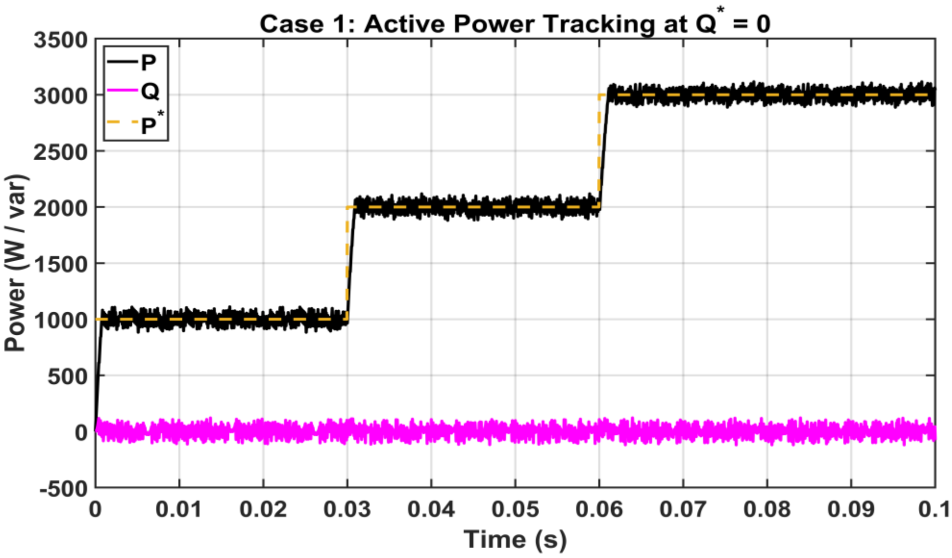

Fig 6 (a): active power and reactive power waveforms under case 1.

Throughout the operation, despite multiple step changes in active power, reactive power remains close to zero. This result shows that the proposed MPDPC method can effectively decouple active and reactive power components in a rotating d-q coordinate system. During the steady-state phase, the active power waveform shows slight fluctuations around the reference value. This is primarily due to the finite control characteristic of the predictive controller, which is, only one voltage vector can be selected from a finite number of inverter switching states at each sampling time. However, the amplitude of this fluctuation remains within an acceptable range and does not affect the overall power point tracking performance.

The three-phase current waveforms shown in Figure 6(b) further confirm the effectiveness of the proposed control strategy. As the active power reference value increases, the amplitude of the grid-connected current increases accordingly. In the first time period $P^* = 1$ kw, the current amplitude is relatively low; when the reference value increases to 2 kw, the current amplitude rises smoothly to match the higher power injection level; after t = 0.06 s, the current amplitude increases further, corresponding to an active power output of 3 kw.

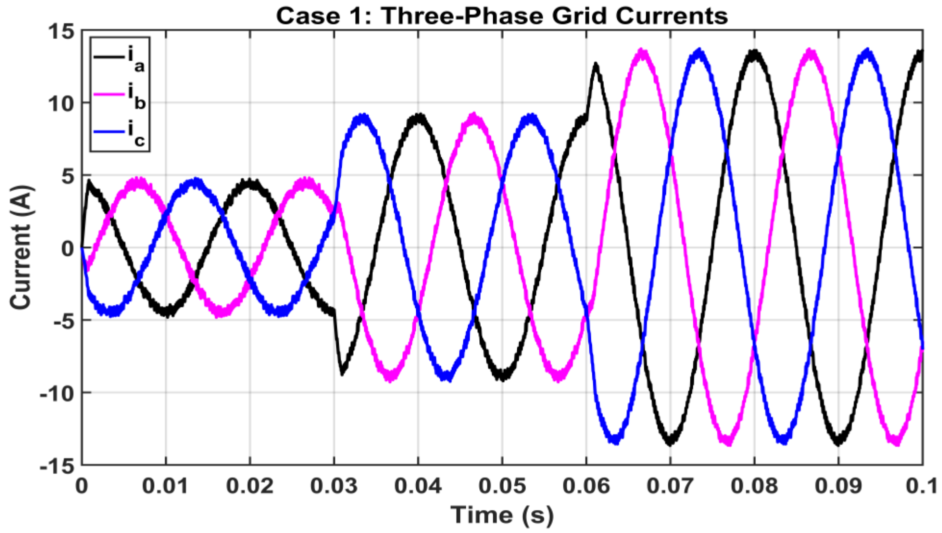

Fig 6(b): three-phase current waveforms.

Case 2: Reactive Power Tracking at $P^* = 0$

Under the second operating case, the aim is to evaluate the dynamic regulation capability of the proposed Model Predictive Direct Power Control (MPDPC) strategy for reactive power. The DC bus voltage is kept at 380V. The reactive power reference $Q^*$is set in different time intervals: 0 kVar for $0 \le t < 0.03$ s, 1 kVar for $0.03 \le t < 0.06$ s, and 2 kVar for $0.06 \le t \le 0.10$ s.

Meanwhile, active power reference is set to $P^* = 0$, To specifically study the independent regulation performance of reactive power. All other system and controller parameters are kept unchanged.

The simulation results are shown in Figures 6(c) and 6(d). Figure 6(c) shows the dynamic response waveforms of active power P and reactive power Q.

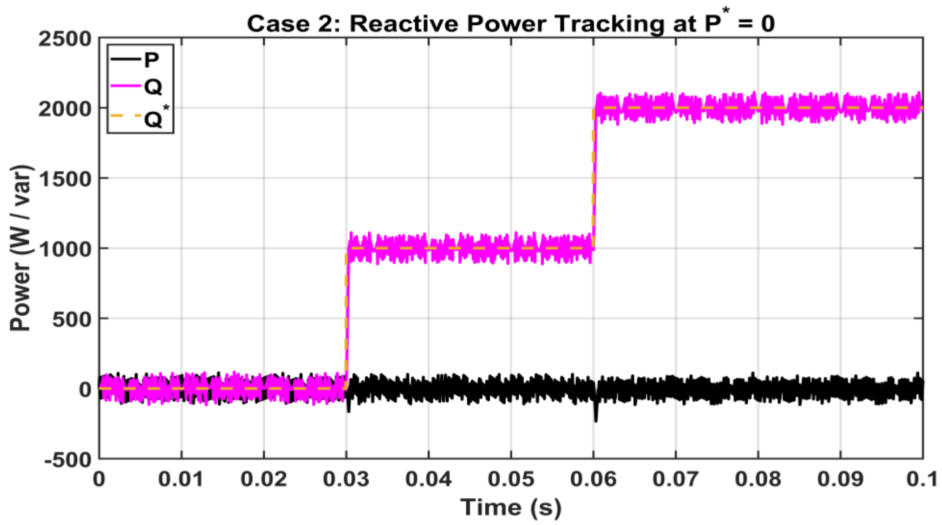

Fig 6(c): Dynamic response waveforms of P and Q.

As can be seen from Figure 6(c), when the reactive power setpoint undergoes a step change, the actual reactive power output can quickly respond and track the reference value. Specifically, at t = 0.03 s and t = 0.06 s, the reactive power steps from 0 kVar to 1 kVar and from 1 kVar to 2 kVar, respectively. The actual reactive power reaches the new setpoint within small time, showing good dynamic tracking performance. Throughout the reactive power regulation process, the active power remains close to zero, further verifying the proposed MPDPC strategy's good active and reactive power decoupling control capability in the d-q coordinate system.

Figure 6(d) shows the three-phase grid-connected current waveforms, further validating the effectiveness of the proposed control strategy. When the reactive power reference value undergoes a step change, the three-phase current can quickly output the corresponding reactive current component to adapt to the new reactive power demand. As the reactive power reference value increases, the current amplitude increases accordingly, and the current waveform remains balanced and sinusoidal throughout the dynamic process, without significant distortion or transient impact.

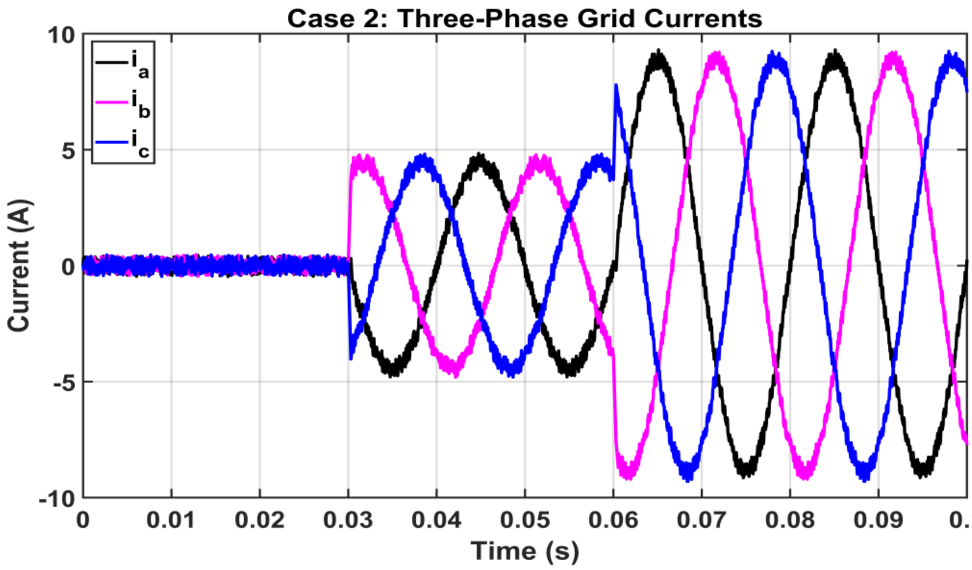

Fig 6(d): three-phase grid-connected current waveforms.

Case 3: Irradiance Variation and Output Power Response

To examine the adaptability of the proposed controller under dynamic photovoltaic power generation conditions, the solar irradiance was increased in a stepwise manner, as shown in Figure 6(e). The irradiance stepped from to , and then further increased to . Corresponding to the change in irradiance, the active power reference value P^* was adjusted based on the photovoltaic power, while the reactive power reference value was set and maintained at a value close to zero.

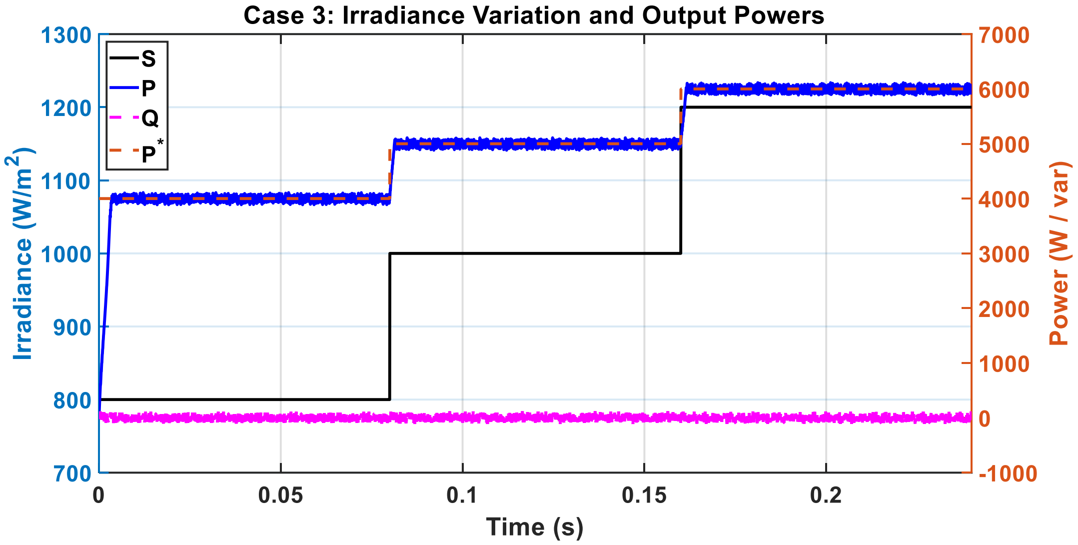

Fig 6(e): (e) Changes in irradiance S and P and Q under.

The simulation result shows that the active power P follows the reference P^*rapidly when the irradiance changes. When the irradiance increases, the available PV power increases, and the inverter output active power rises accordingly. The active power tracks approximately 4 kw, 5 kw, and 6 kw for irradiance levels respectively. This confirms that the proposed MPDPC strategy can respond effectively to variations in solar irradiance.

Throughout the irradiance variation, reactive power remained close to zero, indicating that the inverter primarily injected active power into the grid and operated at approximately unity power factor. Although both active and reactive power exhibited slight fluctuations due to the switching characteristics of the finite control set of the MPDPC strategy, the overall tracking performance remained satisfactory.

Figure 6(f) shows the three-phase grid current waveforms under varying irradiance conditions. The current amplitude increased with increasing irradiance and active power. Throughout the simulation, the three-phase currents remained balanced and the waveforms almost sinusoidal. This result confirms that the proposed controller can maintain stable grid current operation while adapting to changes in photovoltaic output power.

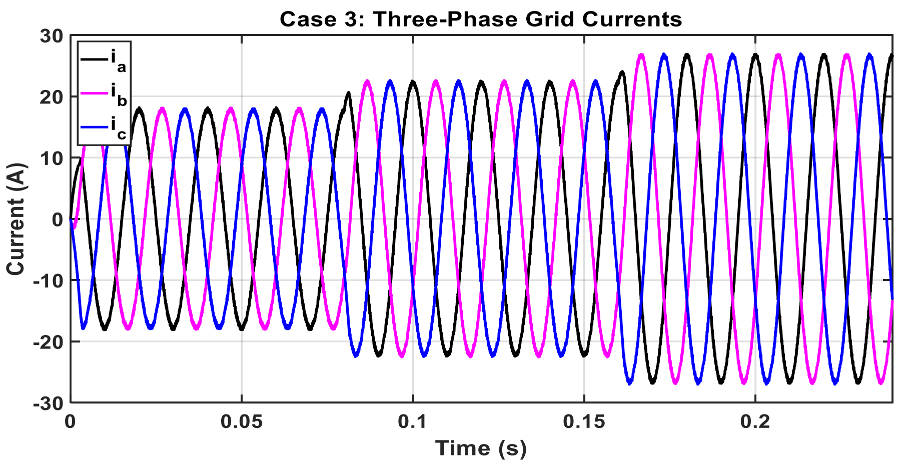

Fig 6(f): Three-phase grid-connected current under case 3.

5. Conclusion

This paper focuses on a three-phase photovoltaic grid-connected inverter in a rotating d-q coordinate system and conducts research on a MPDPC strategy. First, the basic principle of MPC is analyzed, and then a mathematical model of the system in a synchronous rotating d-q coordinate system is established. Based on system simulation studies, the following conclusions are determined:

(1) The proposed MPDPC strategy has good dynamic performance. Under step changes in active and reactive power, the controlled power can track its reference value, with rapid transient response and small steady-state deviation, verifying the advantages of this strategy in power regulation.

(2) The MPDPC strategy has a simple control structure, facilitating algorithm implementation. Since no internal current loop and PWM module are needed, the controller design and parameter tuning process are significantly simplified. Simultaneously, by changing the given reactive power reference value, this control method can effectively compensate for reactive power in the grid, thereby providing voltage support for the grid. (3) This control method enables arbitrary adjustment of the power factor and exhibits good decoupling control characteristics between active power (P) and reactive power (Q).

References

[1] F. Blaabjerg, R. Teodorescu, M. Liserre, and A. V. Timbus, "Overview of control and grid synchronization for distributed power generation systems," *IEEE Transactions on Industrial Electronics*, vol. 53, no. 5, pp. 1398–1409, 2006.

[2] T. Esram and P. L. Chapman, "Comparison of photovoltaic array maximum power point tracking techniques," *IEEE Transactions on Energy Conversion*, vol. 22, no. 2, pp. 439–449, 2007.

[3] S. B. Kjaer, J. K. Pedersen, and F. Blaabjerg, "A review of single-phase grid-connected inverters for photovoltaic modules," *IEEE Transactions on Industry Applications*, vol. 41, no. 5, pp. 1292–1306, 2005.

[4] R. Teodorescu, M. Liserre, and P. Rodriguez, *Grid Converters for Photovoltaic and Wind Power Systems*. Hoboken, NJ, USA: Wiley-IEEE Press, 2011.

[5] M. P. Kazmierkowski and L. Malesani, "Current control techniques for three-phase voltage-source PWM converters: A survey," *IEEE Transactions on Industrial Electronics*, vol. 45, no. 5, pp. 691–703, 1998.

[6] F. Eltoumi, "Charging station for electric vehicle using hybrid sources," Ph.D. dissertation, Université Bourgogne Franche-Comté, France, 2017.

[7] P. Cortés, M. P. Kazmierkowski, R. M. Kennel, D. E. Quevedo, and J. Rodríguez, "Predictive control in power electronics and drives," *IEEE Transactions on Industrial Electronics*, vol. 55, no. 12, pp. 4312–4324, 2008.

[8] S. Kouro, P. Cortés, R. Vargas, U. Ammann, and J. Rodríguez, "Model predictive control—A simple and powerful method to control power converters," *IEEE Transactions on Industrial Electronics*, vol. 56, no. 6, pp. 1826–1838, 2009.

[9] S. Vazquez, J. Rodríguez, M. Rivera, L. G. Franquelo, and M. Norambuena, “Model predictive control for power converters and drives: Advances and trends,” *IEEE Transactions on Industrial Electronics*, vol. 64, no. 2, pp. 935–947, 2017.

[10] J. Rodríguez, M. P. Kazmierkowski, J. R. Espinoza, P. Zanchetta, H. Abu-Rub, H. A. Young, and C. A. Rojas, “State of the art of finite control set model predictive control in power electronics,” *IEEE Transactions on Industrial Informatics*, vol. 9, no. 2, pp. 1003–1016, 2013.

[11] J. Rodríguez and P. Cortés, *Predictive Control of Power Converters and Electrical Drives*. Hoboken, NJ, USA: Wiley-IEEE Press, 2012.

[12] S. N. Thanh, “Predictive direct power control of grid-connected PV systems,” *Mathematical Modelling of Engineering Problems*, 2023.

[13] S. Ahmad, A. Abu-Siada, and M. S. A. Dahidah, “Point of common coupling voltage modulated direct power control for grid-tied photovoltaic voltage source inverter,” 2023.

[14] F. M. Eltoumi, M. Becherif, A. Djerdir, and H. S. Ramadan, “The key issues of electric vehicle charging via hybrid power sources: Techno-economic viability, analysis, and recommendations,” *Renewable and Sustainable Energy Reviews*, vol. 138, Art. no. 110534, 2021.

[15] H. Akagi, E. H. Watanabe, and M. Aredes, Instantaneous Power Theory and Applications to Power Conditioning, 2nd ed. Hoboken, NJ, USA: Wiley-IEEE Press, 2017.

[16] B. Lekouaghet, A. Boukabou, N. Lourci, and K. Bedrine, “Control of PV grid connected systems using MPC technique and different inverter configuration models,” Electric Power Systems Research, vol. 154, pp. 287–298, 2018.

[17] S. Mirza and A. Hussain, “New approaches in finite control set model predictive control for grid-connected photovoltaic inverters: State of the art,” Solar, vol. 4, no. 3, pp. 491–508, 2024.

[18] P. Karamanakos, E. Liegmann, T. Geyer, and R. Kennel, “Model predictive control of power electronic systems: Methods, results, and challenges,” IEEE Open Journal of Industry Applications, vol. 1, pp. 95–114, 2020.

[19] Elwalwa, H. M., Zarig, F. H. A., Murad, M. K. H., & Nashnush, A. N. E. (2026). The role of innovation technology in developing solar energy technologies: challenges and future trends towards sustainable development (literature review). *Al-Farooq Journal of Sciences*, *2*(3), 585-594.

[20] Alriheebi, R. A. (2026). Integrated Modeling and Mult objective Control of Multilevel DC/AC Inverters for Conducted Electromagnetic Interference Mitigation. *Al-Farooq Journal of Sciences*, *2*(3), 897-925.

[21] Jamom, A. M., & Albohli, N. A. (2026). Evaluation of the technical and environmental feasibility of replacing a steam generation unit with wind turbines at the Zawia refinery, Libya. *Al-Farooq Journal of Sciences*, *2*(3), 149-160.

[22] Yakhlef, A. S. A., & Azzabi, A. S. I. (2025). Dynamic Analysis of the West Tripoli Gas Turbine Power Plant Using MATLAB Simulation. *Al-Farooq Journal of Sciences*, *1*(1), 122-135.

[23] Ramadhan, H. R. S., Osman, M. O. M., Dalla, L. O. F. B., Rashid, T. A., Albaraesi, M. J. S., EL-sseid, M. A. M., & Alnnale, T. (2025). A New Approach of the Machine Learning Framework Integrating Policy Design to Predict Renewable Electricity Penetration in Resource-Constrained Settings. *مجلة العلوم الشاملة*, *10*(ملحق 38), 2929-2950.